

# Regenerative Braking for EVs Using PMSM with CHB as Bidirectional Traction Converter

Fatemeh Nasr Esfahani

*Engineering Department  
Lancaster University  
Lancaster, LA1 4YW, UK*

f.nasresfahani@lancaster.ac.uk

Ahmed Darwish

*Engineering Department  
Lancaster University  
Lancaster, LA1 4YW, UK*

a.badawy@lancaster.ac.uk

**Abstract-** Permanent-magnet synchronous motor (PMSM) is broadly adopted in electric vehicles (EVs) due to its superior advantages like providing high efficiency and excellent torque-speed characteristics. Regenerative braking (RB), which is the recovery of the kinetic energy during deceleration, is an efficient method to restore the kinetic energy into the battery to extend the battery and hence the driving range. In this paper, an RB strategy is proposed where the drive shaft's torque is estimated using a detailed analysis of all the forces acting on an EV along an inclined road. To achieve the maximum electromagnetic torque, the d-axis component of the stator current is set to zero. Then, the three-phase voltages are generated and applied to the stator windings based on the EV demand. To improve the harmonic performance, the multilevel cascaded half-bridge (CHB) converter is used as the bidirectional traction converter. The proposed RB strategy is verified in the operating modes of acceleration, deceleration (braking), and constant speed using MATLAB/Simulink computer simulations and tested with a small-scale experimental rig controlled by TMSF28335 Digital Signal Processor.

**Index Terms – Regenerative Braking (RB), Permanent Magnet Synchronous Machine (PMSM), Electric Vehicles (EVs), Multilevel Converters, Cascaded Half-Bridge (CHB).**

## I. INTRODUCTION

Based on the transport and environment annual report in 2021, the transport sector has been the major producer of greenhouse gas (GHG) emissions, generating 27% of the UK's total emissions in 2019. Therefore, road transport, including passenger cars, light commercial vehicles, and heavy-duty vehicles, is emitting 122 million tonnes of CO<sub>2</sub> equivalent (MtCO<sub>2</sub> e) [1]. Besides, the demand for gasoline and diesel in Europe (EU) has been unceasingly rising since 1990. Electric vehicles (EVs) can substantially reduce GHG emissions and gasoline consumption. EVs can be broadly broken into battery electric vehicles (BEVs), hybrid electric vehicles (HEVs), and plug-in hybrid electric vehicles (PHEVs). While HEVs and PHEVs are powered by both petrol/diesel and electricity, BEVs are powered entirely by electricity and hence are known as pure EVs [2].

The fundamental components of a BEV are the electric propulsion system, high voltage (HV) battery pack, low voltage (LV) battery system, transmission system, and battery charger (typically an AC-DC converter followed by an isolated

DC-DC converter) [2]. The electric propulsion system itself contains an electric motor (AC or DC) and a traction converter. DC motors used to be the most dominant in primary EV propulsion systems for a long period [3]. Nevertheless, they suffer from low power density, low efficiency, and the problems associated with the carbon brushes. Instead, induction motors (IM), permanent magnet synchronous machines (PMSM), and brushless DC machines (BLDC) have turned into the most common motors considering the advancement in their features. The PMSM can deliver benefits like reduced motor size and high torque-to-volume ratio. In practice, PMSM has proved that it can provide high efficiency at high speeds, high reliability, full torque at low speeds, and smooth dynamic performance [3].

Looking at the EV's power converters, multi-level converters, including Neutral-Point Clamped (NPC), Flying Capacitor (FC), Cascaded H-bridge (CHB), and Modular multi-level converters (MMC), generate staircase voltage waveform at the AC side and are promising candidates in motor drives as the intermediate bidirectional traction converter. They offer lower total harmonic distortion (THD), higher efficiency, less voltage stress on semiconductor devices, near-sinusoidal currents at the AC side (in rectifier operation) in addition to smaller filters at both AC and DC sides [4].

Limited driving and battery range, high costs, low efficiency, low power density, and charging infrastructures are the main issues facing the progress of BEVs [2].

Integration of renewable energies (e.g., solar [5-6]) into EVs and regenerative braking (RB) are promising solutions to address these issues. With RB, the kinetic energy is converted into electricity which can be either used immediately or stored until needed [7-8].

In recent years, a numerous research publications have considered regenerative braking systems (RBS) of PMSM used for EVs [9-20]. The control strategy implemented in the RBS, such as super capacitor energy storage [13] and electric braking [14], is the main factor affecting the amount of energy recovered. Instead of using batteries, an RBS system utilizing a PMSM as the propulsion unit is utilized in [15], resulting in higher efficiency and a higher torque density. A control strategy for the RBS is put forward in [16] which can raise the efficiency to 60%. Supercapacitors and ultracapacitors, on the

other hand, would allow recovering energy from braking up to 20 times more than that of conventional batteries at any speed and for any distance [17-18]. To develop accurate RBS models to be inserted in simulators, authors in [19] focused on RBS modelling rather than designing and implementing new RB strategies. However, the voltage source inverter (VSI) is mostly used as the traction converter in these studies. The VSI utilizes the full HV battery pack and causes high THD, which calls for large electrolytic capacitors at the AC side [21-22].

In this paper, the drive shaft's torque is estimated using a detailed analysis of all the forces acting on an EV along an inclined road. The d-axis and q-axis components of the stator current are used to control the rotor flux linkage and the motor torque, respectively. Eventually, the three-phase voltages are generated and applied to the stator windings based upon the demand of the vehicle. The multilevel CHB is used as the bidirectional traction converter due to its superb advantages mentioned earlier. The rest of this paper is organized as follows: the dynamic modelling of the PMSM and the general concept of RB are presented in Sections II and III, respectively. After a brief review of the pros and cons of multilevel converters in Section IV, the proposed RB strategy is discussed in Section V. Verifications are provided in Section VI by simulations and experiments. Finally, this paper is concluded in Section VII.

## II. PMSM DYNAMIC MODELLING

PMSM (also known as brushless AC motor (BLAC)) is an AC machine whose stator is excited by three-phase sinusoidal AC currents while its rotor is a permanent magnet, providing the customers with advantages like reduced motor size and a more straightforward structure. In practice, PMSM has proved that it can deliver higher efficiency at high speeds and higher reliability. Moreover, it is capable of maintaining full torque at low speeds. These advantages and many others have made this motor a promising candidate for applications like EVs [3].

To extract the dynamic model of the PMSM, let us consider the three-phase sinusoidal voltages applied to stator windings as:

$$\begin{cases} v_a(t) = V_m \sin(\omega t) \\ v_b(t) = V_m \sin(\omega t - \frac{2\pi}{3}) \\ v_c(t) = V_m \sin(\omega t + \frac{2\pi}{3}) \end{cases} \quad (1)$$

, where  $V_m$  is the phase voltage amplitude and  $\omega (=2\pi f)$  is the angular frequency. The d-q model is developed on a rotor reference frame, where at any time  $t$ , the rotating rotor q-axis makes an angle  $\theta_e$  with the fixed stator phase axis [23]. After applying the generalized Park Transformation Matrix as:

$$[T^{qd0}(\theta_e)] = \sqrt{\frac{2}{3}} \begin{bmatrix} \cos(\theta_e) & \cos(\theta_e - \frac{2\pi}{3}) & \cos(\theta_e + \frac{2\pi}{3}) \\ \sin(\theta_e) & \sin(\theta_e - \frac{2\pi}{3}) & \sin(\theta_e + \frac{2\pi}{3}) \\ \frac{1}{2} & \frac{1}{2} & \frac{1}{2} \end{bmatrix} \quad (2)$$

, the state equations can be calculated in the d-q rotor reference frame as:

$$\begin{aligned} [v^{qd0}] &= [T^{qd0}(\theta_e)] [v^{abc}] \\ &= [R_s^{qd0}] [i_s^{qd0}] + \frac{d}{dt} ([\lambda_s^{qd0}]) + [T^{qd0}(\theta_e)] \cdot \frac{d}{dt} ([T^{qd0}(\theta_e)]^{-1}) \cdot [\lambda_s^{qd0}] \\ &= [R_s^{qd0}] [i_s^{qd0}] + \frac{d}{dt} ([\lambda_s^{qd0}]) + [T^{qd0}(\theta_e)] \cdot \frac{d}{d\theta_e} ([T^{qd0}(\theta_e)]^{-1}) \cdot \frac{d\theta}{dt} \cdot [\lambda_s^{qd0}] \\ &= [R_s^{qd0}] [i_s^{qd0}] + \frac{d}{dt} ([\lambda_s^{qd0}]) + \omega_e \begin{bmatrix} 0 & 1 & 0 \\ -1 & 0 & 0 \\ 0 & 0 & 0 \end{bmatrix} \cdot [\lambda_s^{qd0}] \end{aligned} \quad (3)$$

, so q- and d-axis voltages can be written as:

$$\begin{cases} v_q = R_s i_q + \frac{d}{dt} \lambda_q + \omega_e \lambda_d \\ v_d = R_s i_d + \frac{d}{dt} \lambda_d - \omega_e \lambda_q \end{cases} \quad (4)$$

, where:

$$\begin{cases} \lambda_q = L_q i_q \\ \lambda_d = L_d i_d + \lambda_m \end{cases} \quad (5)$$

, with  $\lambda_q$  and  $\lambda_d$  being q- and d-axis flux linkages, respectively.  $L_q$  and  $L_d$  represent stator inductances in the q-axis and d-axis, respectively.  $R_s$  indicates stator winding resistance,  $\omega_e$  is the electrical angular frequency, and  $\lambda_m$  represents the flux linkage induced by the rotor magnets linking the stator.

The general mechanical equation for the PMSM motor is as:

$$T_e - T_L = B\omega_m + J \frac{d\omega_m}{dt} \quad (6)$$

, where the electromagnetic torque  $T_e$  is given by [23]:

$$T_e = \frac{3}{2} \frac{P}{2} (\lambda_d i_q - \lambda_q i_d) = \frac{3}{2} \frac{P}{2} (\lambda_m i_q + (L_d - L_q) i_d i_q) \quad (7)$$

, with  $T_L$ ,  $B$ ,  $\omega_m$ , and  $J$  being shaft (load) torque, viscous friction coefficient, mechanical velocity, and inertia of the shaft and the load system, respectively. The relation between the electrical velocity  $\omega_e$ , mechanical velocity  $\omega_m$ , and the rotating rotor q-axis angle  $\theta_e$  (with respect to the fixed stator phase axis) can be expressed as:

$$\begin{cases} \omega_e = \frac{P}{2} \omega_m \\ \theta_e = \int \omega_e(t) dt \end{cases} \quad (8)$$

, with  $P$  being the number of rotor poles.

## III. REGENERATIVE BRAKING (RB) GENERAL CONCEPT

During friction braking, a majority of kinetic energy is converted into heat and emitted unused to the environment.

However, EVs with RB can recover the kinetic energy to the electricity and store it until needed, extending the battery and the driving range [7]. The typical structure of a battery EV (BEV) with acceleration and RB (deceleration) modes is shown in Fig. 1. Controllers, motors, converters, the traction system (gearbox, differentials, etc.), and high-voltage (HV) and low-voltage (LV) battery boxes are common components in BEVs. The red and blue arrows are used in this figure to represent the flow of the power during “driving mode” (from the HV battery box to the motor) and “RB mode” (from the motor to the HV battery box), respectively.

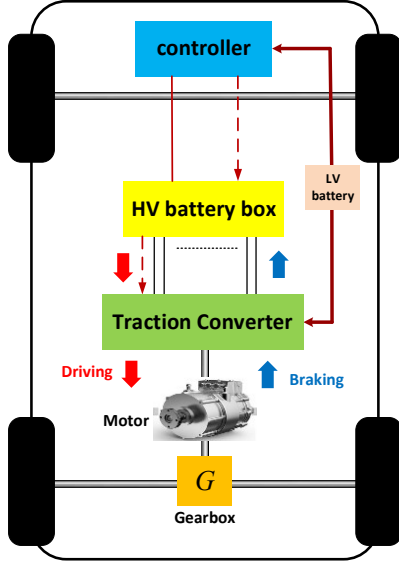


Fig. 1. Typical structure of BEVs with driving (motoring) and regenerative modes

#### IV. MULTILEVEL CONVERTERS

Multilevel topologies, including Neutral-Point Clamped (NPC), Flying Capacitor (FC), Cascaded H-bridge (CHB), and Modular multi-level converters (MMC), produce staircase voltage waveform at the AC side, leading to less total harmonic distortion (THD). They are extensively used in motor drives as they offer higher efficiency, lower voltage stress on semiconductor switches, near-sinusoidal currents at the AC side (in rectifier operation) and smaller filters at both AC and DC sides [4]. A brief comparison is made between the multilevel topologies and presented in TABLE I.

#### V. THE PROPOSED RB STRATEGY

The block diagram of the proposed RB strategy using the PMSM is displayed in Fig. 2. As can be seen, the reference velocity profile is used to generate the reliable value of drive shaft torque  $T_L$  and hence the reference d- and q-axis voltages ( $v_{dref}$  and  $v_{qref}$ ). After applying the inverse Park Transformation Matrix, the reference phase voltages  $v_{aref}$ ,  $v_{bref}$ , and  $v_{cref}$  are generated and applied to the stator windings. The multilevel CHB is employed as the bidirectional traction converter due to its superb advantages listed in TABLE I. More details on the proposed RB strategy are presented in the subsections.

TABLE I

KEY BENEFITS AND CHALLENGES OF DIFFERENT MULTILEVEL TOPOLOGIES [4]

Topology	Benefits	Challenges
<b>NPC</b>	<ul style="list-style-type: none"> <li>✓ Simple topology</li> <li>✓ Simple PWM technique</li> <li>✓ Zero-sequence injection to control the DC voltage imbalance</li> </ul>	<ul style="list-style-type: none"> <li>✗ Unequal usage of power devices</li> <li>✗ DC-link voltage balance required</li> </ul>
<b>FC</b>	<ul style="list-style-type: none"> <li>✓ Natural floating DC voltages balance</li> <li>✓ Super harmonic performance</li> <li>✓ Fault-tolerant capability</li> </ul>	<ul style="list-style-type: none"> <li>✗ Poor dynamic response of the natural DC voltage balancing</li> <li>✗ High number of floating voltages</li> </ul>
<b>CHB</b>	<ul style="list-style-type: none"> <li>✓ <b>Mature technology</b></li> <li>✓ <b>Commercialized by several companies</b></li> <li>✓ <b>Fault-tolerant capability</b></li> <li>✓ <b>Straightforward extension to achieve a high number of levels</b></li> <li>✓ <b>Equal power distribution</b></li> <li>✓ <b>Superior harmonic performance</b></li> <li>✓ <b>Lower design and control complexity</b></li> </ul>	<ul style="list-style-type: none"> <li>✗ <b>Each H-bridge requires an isolated DC source</b></li> </ul>
<b>MMC</b>	<ul style="list-style-type: none"> <li>✓ Formed by the series connection of simple power cells</li> <li>✓ Fault-tolerant capability</li> <li>✓ Simple gate driver generation method</li> <li>✓ Average equalization of power losses and floating DC voltages balance</li> </ul>	<ul style="list-style-type: none"> <li>✗ Complex data acquisition and communication</li> <li>✗ Complex hardware to operate the converter</li> </ul>

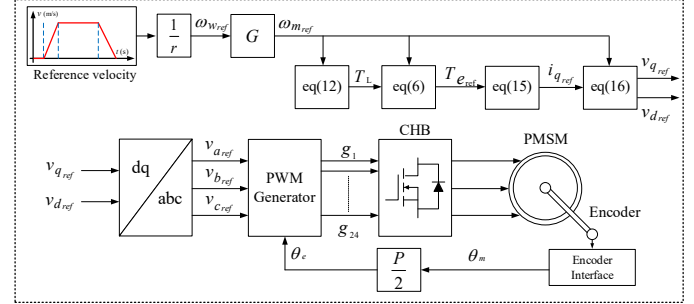


Fig. 2. The proposed RB strategy using PMSM with CHB as the bidirectional traction converter

#### A. EV dynamic modelling

For an EV travelling along an inclined road, the velocity profile and the associated resistance forces are demonstrated in Fig. 3(a) and (b), respectively.

The total force  $F_{te}$  (tractive effort) required from this EV is equal to the sum of the friction force  $F_{rr}$ , the hill-climbing force  $F_{hc}$ , the aerodynamic force  $F_{ad}$ , and the acceleration force  $F_{la}$ , as follows:

$$F_{te} = F_{rr} + F_{hc} + F_{ad} + 1.05F_{la} \quad (9)$$

, where:

$$\begin{cases} F_{rr} = \mu_r mg \\ F_{hc} = mg \sin(\psi) \\ F_{ad} = \frac{1}{2} \rho AC_d v^2 \\ F_{la} = ma \end{cases} \quad (10)$$

, with  $\mu_r$ ,  $\psi$ ,  $g$ , and  $\rho$  being rolling resistance coefficient, the inclination of road surface, acceleration due to gravity, and density of air, respectively. The parameters  $v$ ,  $a$ ,  $A$ ,  $C_d$ , and  $m$  stand for speed, acceleration, frontal area, drag coefficient, and vehicle mass, respectively.

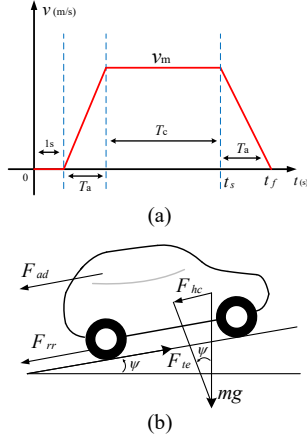


Fig. 3. EV along an inclined road (a) velocity profile of EV (b) associated resistance forces

Given that torque is a particular form of force that turns an axle in a given direction, torque at the wheel side  $T_w$  is equal to  $T_w = r.F_{te}$ , with  $r$  being the wheel radius. In addition, there is a gearbox with the gear-ratio  $G$  located between the motor and the wheel, which is responsible for capturing the rotational motion of the motor and distributing this motion to the two rear wheels (see Fig. 4). Therefore, it can be expected that the speed at the motor side  $\omega_m$  to be higher than the speed at the wheel side  $\omega_w$  (since  $G.\omega_w = \omega_m$ ).

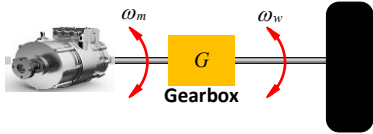


Fig. 4. The gearbox with the gear-ratio  $G$  located between the motor and wheel

Finally, the required shaft's torque along an inclined road at the motor side  $T_m$  can be calculated as:

$$\begin{aligned} T_m &= \frac{mgr(\mu_r + \sin(\psi))}{G} + \frac{1}{2G^3} \rho AC_d \omega_m^2 r^3 + \frac{1.05mr^2 \alpha_m}{G^2} \\ &= T_F + K_d \omega_m^2 + J_m \alpha_m \end{aligned} \quad (11)$$

, with  $\omega_m$  and  $\alpha_m$  being the angular speed and acceleration, respectively.

## B. RB using PMSM

For the general torque equation of the PMSM in (6), the electromagnetic torque is as (7), and the required drive shaft torque  $T_L$  is equal to:

$$T_L = T_F + K_d \omega_m^2 \quad (12)$$

, where the constants  $T_F$  and  $K_d$  are defined as:

$$\begin{cases} T_F = \frac{\mu_r mgr}{G} \\ K_d = \frac{1}{2G^3} \rho AC_d r^3 \end{cases} \quad (13)$$

In the rotor flux-oriented coordinate system, the d-axis component of the stator current  $i_d$  is used to control the rotor flux linkage, and the q-axis component  $i_q$  is used to control the motor torque. Therefore, the maximum electromagnetic torque  $T_{e(max)}$  can be achieved by setting the control variable  $i_d$  equal to zero:

$$T_{e(max)} = \frac{3P}{2} \left( \lambda_m i_q \right) \quad (14)$$

, therefore, the reference value of the q-axis current and d-q axis voltage equations can be extracted as (15) and (16), respectively:

$$i_{q(ref)} = \frac{4}{3P} \left( \frac{T_{e(max)}}{\lambda_m} \right) \quad (15)$$

$$\begin{cases} V_d = -\omega L_q i_{q(ref)} \\ V_q = r i_{q(ref)} + \omega \lambda_m \end{cases} \quad (16)$$

Finally, the inverse Park Transformation Matrix can be used to calculate the reference phase voltages  $v_{aref}$ ,  $v_{bref}$ , and  $v_{cref}$ .

## VI. VERIFICATION

### A. Simulation study

The proposed RB strategy is implemented in Simulink/MATLAB environment using the parameters listed in TABLE II. Simulations are carried out using a voltage source inverter (VSI) and CHB as the bidirectional traction converter and compared to show the effectiveness of the CHB in terms of harmonic performance.

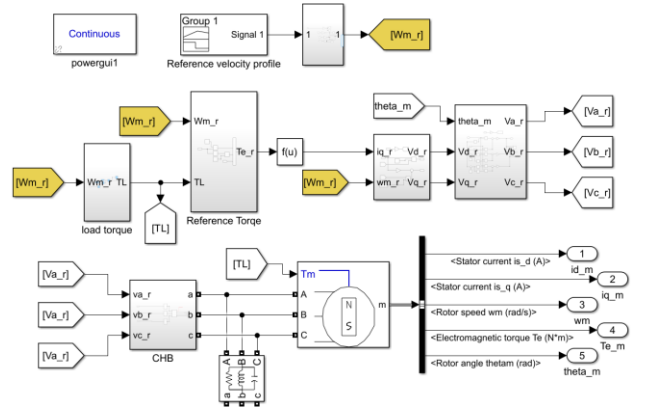


Fig. 5. Block diagram of RB using PMSM in MATLAB/Simulink

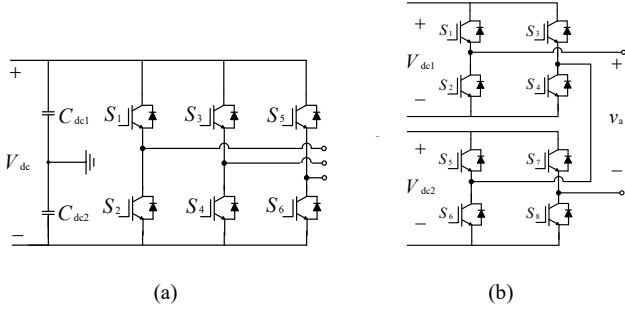


Fig. 6. Traction converter (a) VSI (b) CHB (phase a)

TABLE II  
PARAMETERS VALUES IN SIMULINK/MATLAB

Parameter	Value
Mass	$m=30\text{kg}$
Gear ratio	$G=5$
Wheel radius	$r=0.3\text{m}$
Rolling resistance coefficient	$\mu_{rr} = 0.05$
Drag Coefficient	$C_d=0.05$
Frontal Area	$A=1\text{m}^2$
Air density	$\rho = 1.225\text{kg/m}^3$
Gravity	$g=9.8\text{m/s}^2$
Linkage flux	$\lambda_m = 0.2\text{Wb-t}$
Viscous friction coefficient	$B=0.014$
Stator winding resistance	$R_s=0.6\Omega$
Shaft inertia	$J=0.02\text{kg.m}^2$
d-axis stator inductance	$L_d=1.4\text{mH}$
q-axis stator inductance	$L_q=2.8\text{mH}$
Rotor poles	$P=2$
Switching frequency	$f_s=1\text{kHz}$

Fig. 7(a) and (b) show the stator windings three-phase voltages ( $v_a(t)$ ,  $v_b(t)$ , and  $v_c(t)$ ) using VSI and CHB, respectively. As can be seen, the three-phase voltages for CHB are much closer to sinusoidal compared to their VSI counterparts.

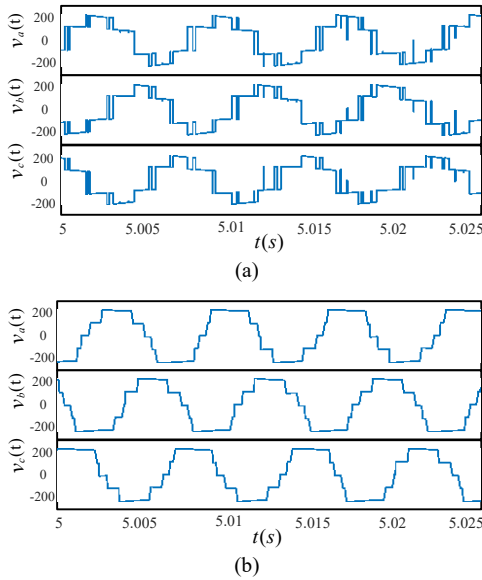


Fig. 7. Simulation results for RB using PMSM: (a) Stator windings three-phase voltages with VSI and (b) with CHB

The simulation results for the rotor speed  $\omega_m$ , q-axis currents  $i_q$ , and electromagnetic torque  $T_e$  are shown in Fig. 8 (a)-(f). As can be seen, the actual value of the rotor speed  $\omega_m$  (in red line) is tracking its reference value (in blue line) in the operating modes of zero speed, acceleration, constant speed, and deceleration (braking), especially when the CHB is used as the traction converter.

As for the electromagnetic force  $T_e$ , the torque is zero during the first 1sec since the rotor speed  $\omega_m$  is zero (the EV is not moving). When the car is accelerating, the torque is increasing as well.  $T_e$  is then constant and less than its previous value as the EV is only being pushed in the same direction. Finally, the electromagnetic force  $T_e$  is negative during deceleration or RB.

The q-axis current  $i_q$  is tracking its reference value. As can be seen in Fig. 8(e) and (f), it is also negative during RB, meaning that the current direction is reversed and the energy is now transferring from the motor to the battery. This is exactly what is called the action of RB.

In addition, Fig. 9 shows the Fast-Fourier Transform (FFT) of the phase-A current of the PMSM using VSI and CHB converters. As can be seen, the simulations using CHB result in lower THD.

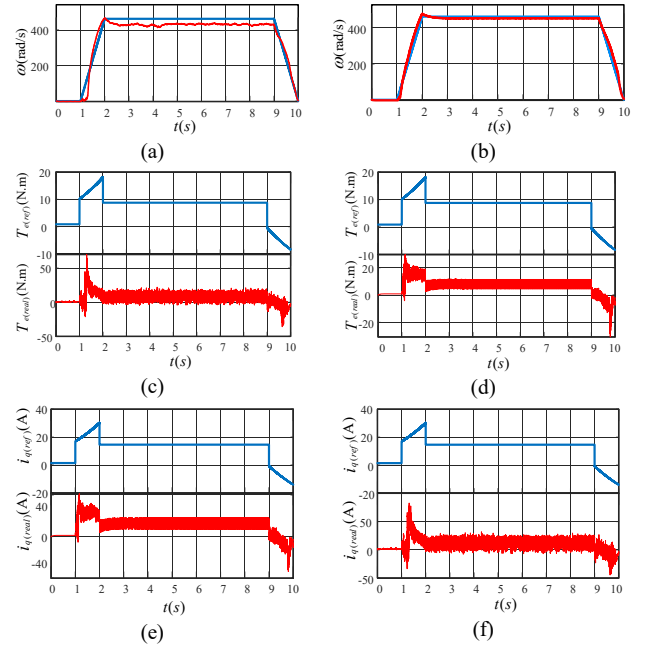


Fig. 8. Simulation results for RB using PMSM: (a) Rotor speed  $\omega_m(\text{rad/s})$  with VSI (b) Rotor speed  $\omega_m(\text{rad/s})$  with CHB (c) Electromagnetic torque  $T_e(\text{N.m})$  with VSI (d) Electromagnetic torque  $T_e(\text{N.m})$  with CHB (e) q-axis current  $i_q(\text{A})$  with VSI (f) q-axis current  $i_q(\text{A})$  with CHB

### B. Experimental results

The small-scale prototype shown in Fig. 10 is used to operate an EMRAX208 PMSM coupled with a mechanical transmission system via a mechanical differential. The CHBs are supplied from 100V battery segments to show both driving and braking modes. Fig. 11(a) shows the rotational speed of the motors when it accelerates from standstill to the maximum speed in 1sec, continues at the

maximum speed for 8sec, and then decelerates in 1sec. Fig. 11(b) shows the currents supplied from the batteries. The negative current during deceleration denotes the RB mode when the power is reversed to charge the battery segments.

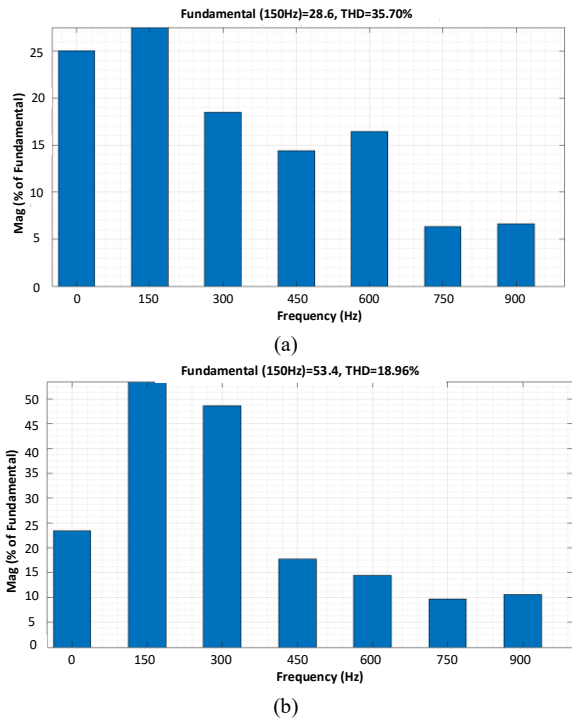


Fig. 9. FFT of the stator phase-A current using (a) VSI and (b) CHB

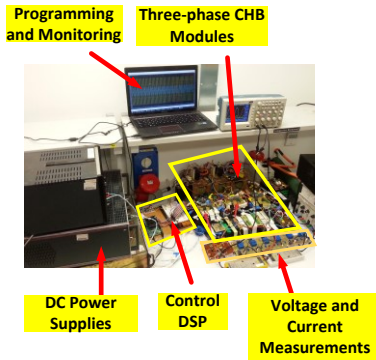


Fig. 10. Experimental set-up

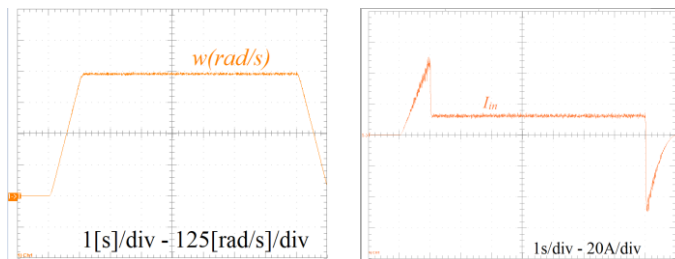


Fig. 11. Experimental results using CHB: (a) Rotor speed  $\omega_m$ (rad/s) and (b) Input CHB current

## VII. CONCLUSION

RB, which is the recovery of kinetic energy during braking (deceleration), can assist EVs to restore the kinetic energy during braking into the battery. Thus, the battery range and the driving range will be extended. After PMSM dynamic modelling, an RB strategy is presented in this paper which estimates the shaft torque using a detailed analysis of all the forces affecting an EV along an inclined road. Then, the three-phase stator winding voltages are generated based on the EV demand. The d-axis and q-axis components of the stator current are used to control the rotor linkage flux and motor torque, respectively. The proposed strategy is verified in all the operating modes of acceleration, deceleration (braking), and constant speed by simulations and experiments. The use of CHB provides better utilization of the battery segments and improves the reliability of the EV. Moreover, the harmonic distortion in the output current is improved using the CHB converter as the bidirectional traction converter which in turn will improve the efficiency.

## REFERENCES

- [1] Hu, Patricia, et al. "Transportation Statistics Annual Report 2021." (2021).
- [2] A. Khaligh and M. D'Antonio, "Global trends in high-power on-board chargers for electric vehicles," *IEEE Transactions on Vehicular Technology*, vol. 68, no. 4, pp. 3306-3324, 2019.
- [3] A. Karki, S. Phuyal, D. Tuladhar, S. Basnet, and B. P. Shrestha, "Status of pure electric vehicle power train technology and future prospects," *Applied System Innovation*, vol. 3, no. 3, p. 35, 2020.
- [4] J. I. Leon, S. Vazquez, and L. G. Franquelo, "Multilevel converters: Control and modulation techniques for their operation and industrial applications," *Proceedings of the IEEE*, vol. 105, no. 11, pp. 2066-2081, 2017.
- [5] M. Niroomand and F. Nasr Esfahani, "Converter Technologies for PV Systems: A Comprehensive Review," In S. M. Tripathi, and S. Padmanaban (Eds.), *Energy Conversion Systems: An Overview*. (Energy Science, Engineering and Technology). Nova Science Publishers, pp. 1-58, 2021.
- [6] T. Shiramagond and W. Lee, "Integration of Renewable Energy into Electric Vehicle Charging Infrastructure," *2018 IEEE International Smart Cities Conference (ISC2)*, pp. 1-7, 2018.
- [7] A. Adib and R. Dhaouadi, "Performance analysis of regenerative braking in permanent magnet synchronous motor drives," *Advances in Science, Technology and Engineering Systems Journal*, vol. 3, no. 1, pp. 460-466, 2018.
- [8] H. Qi, Y. Zhang, and N. Gao, "Research and implement of PMSM regenerative braking strategy based on controllable rectification," *2015 IEEE 11th International Conference on Power Electronics and Drive Systems*. pp. 289-294, 2015.
- [9] C. Qiu, G. Wang, "New evaluation methodology of regenerative braking contribution to energy efficiency improvement of electric vehicles," *Energy Conversion and Management*, pp. 389-398, 2016.
- [10] Y. Zhang, W. Wang, C. Yang, L. Han, Z. Zhang, and J. Liu, "An effective regenerative braking strategy based on the combination algorithm of particle swarm optimization and ant colony optimization for electrical vehicle," *2019 IEEE 28th International Symposium on Industrial Electronics. ISIE*, pp. 1905-1910, 2019.
- [11] C. Li, C. He, Y. Yuan, and J., Zhang, "Control, modeling and simulation on a novel regenerative brake system of electric vehicle," *2018 IEEE 4th International Conference on Control Science and Systems Engineering, ICCSSE*, pp. 90-94, 2018.
- [12] L. Li, Y. Zhang, C. Yang, B. Yan, and C. M. Martinez, "Model predictive control based efficient energy recovery control strategy for

- regenerative braking system of hybrid electric bus,” *Energy Conversion and Management*, pp. 299–314, 2016.
- [13] K. K. Zhang, J. Q. Li, Y. Ou, G. Ming, J. Gu, Y. Ma, “Electric braking performance analysis of PMSM for electric vehicle applications,” *Proceedings of 2011 International Conference on Electronic & Mechanical Engineering and Information Technology*, vol.5, pp.2596-2599, 2011.
- [14] C. Goia, L. Popa, C. Popescu, and M. O. and Popescu, “Supercapacitors used as an energy source to drive the short urban electric vehicles,” *2011 7th International Symposium on Advanced Topics in Electrical Engineering (ATEE)*, vol. pp.1-6, 2011.
- [15] Q. Gao, C. Lv, N. Zhao, H. Zang, H. Jiang, Z. Zhang, and F. Zhang, “Regenerative braking system of PM synchronous motor,” *AIP Conference Proceedings*, vol. 1955, no. 1, p. 040111, 2018.
- [16] G. Yanan, “Research on electric vehicle regenerative braking system and energy recovery,” *International Journal of Hybrid Information Technology*,” vol. 9, no. 1, pp. 81-90, 2016.
- [17] S. S. Gopinathan, I. P. Akshara, M. Gibi, M. Jamshad, and V. P. Sadique, “Electrical vehicle with regenerative braking system by using super capacitors,” *International Journal of Electrical and Electronics Research*, vol. 3, no. 2, pp. 188-121, 2015.
- [18] S. K. Malode and R. Adware, “Regenerative Braking System in Electric Vehicles,” *International Research Journal of Engineering and Technology (IRJET)*, vol. 3, no. 3, pp. 394-400, 2016.
- [19] R. Maia, J. Mendes, R. Araújo, M. Silva, and U. Nunes, “Regenerative braking system modelling by fuzzy Q-Learning,” *Engineering Applications of Artificial Intelligence*, pp. 103712, 2020.
- [20] F. Nasr Esfahani, “Regenerative braking using permanent magnet synchronous machine,” *Lancaster University Engineering Department Postgraduate Research Conference*, 2021.
- [21] A. Darwish, A. K. Abdelsalam, A. M. Massoud and S. Ahmed, “Single phase grid connected current source inverter: Mitigation of oscillating power effect on the grid current,” *IET Conference on Renewable Power Generation (RPG 2011)*, pp. 1-7, 2011.
- [22] A. D. Badawy, A. M. Massoud, D. Holliday, and A. Ahmed, “Generation, performance evaluation and control design of single-phase differential-mode buck-boost current-source inverters,” *IET Renewable Power Generation*, vol. 10, no. 7, pp. 916-927, 2016.
- [23] H. M. El Shewy, F. E. Abd Al Kader, M. M. El Kholy, and A. El Shahat, “Dynamic modeling of permanent magnet synchronous motor using MATLAB-simulink,” *International Conference on Electrical Engineering ICEENG*, vol. 6, no. 6, pp. 1-16, 2008.